ACS OMEGA

Open Access

http://pubs.acs.org/journal/acsodf

Article

Antioxidant Activity of $MgSO_4$ Ion Pairs by Spin-Electron Stabilization of Hydroxyl Radicals through DFT Calculations: Biological Relevance

Miguel Fernández,* Reinaldo Marín, and Fernando Ruette

Cite This: *ACS Omega* 2024, 9, 36640−36647

Read Online

ACCESS | Metrics & More | Article Recommendations

ABSTRACT: Magnesium sulfate has been of great interest as an antioxidant for its ability to decrease the oxidizing capacity of the hydroxyl radical. Previously, it was shown that the contact ion pair of this salt could stabilize •OH by coordinating with Mg and delocalizing the unpaired electron over sulfate. The present study explores in detail the $MgSO_4$ antioxidant properties, considering all its ion pairs with •OH in different conformations. The analyses were based on structural, spin, and energetic properties using the DFT approach. As a result, the high antioxidant potential of $MgSO_4$ is related to the spin-electron transfer from SO_4^{-2} to •OH causing electron spin delocalization and electrostatic stabilization. This transfer occurs for all ion pairs when •OH approaches the Mg first solvation shell, without being coordinated to Mg. The direct Mg−•OH interaction further stabilizes the radical system. These results show that spin-electron transfers are feasible in all hydrated ion pairs $MgSO_4$−•OH, even at a •OH−sulfate distance greater than 10 Å.

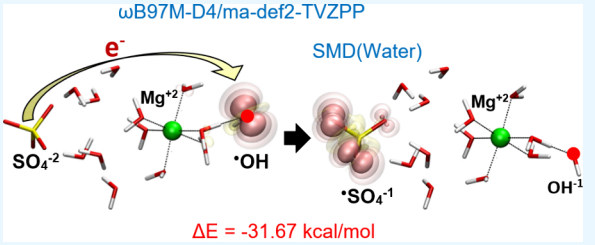

1. INTRODUCTION

Oxidative stress is defined as the alteration of the balance between antioxidant and pro-oxidant species in favor of the latter. It has been intensively studied in recent decades to understand the reaction mechanisms associated with various pathologies such as cancer, cardiovascular, several neurological (i.e., Parkinson's, Alzheimer's), chronic obstructive pulmonary, rheumatoid arthritis disease, and aging, among others.[1,2] The increased levels of reactive oxygen species (ROS)[3] can induce modifications in DNA, RNA, carbohydrates, lipids, and proteins, altering their biological functions. Lipids are one of the species that are most susceptible to ROS attack and oxidative damage induced by lipid peroxidation (LP).[4]

Magnesium and its salts are involved in various biological processes, including carbohydrate metabolism, protein synthesis, DNA replication, stability and repair, nerve function, muscle contraction, and blood pressure regulation. Magnesium has also been found to induce osteoblast proliferation, prevent vascular calcification, enhance antioxidant capacity, reduce mitochondrial ROS production, and improve cellular energy supply and longevity.[5−7]

Magnesium sulfate ($MgSO_4$) is a divalent salt that associates as an ion pair in aqueous solutions. This salt has aroused great interest in the last decades by various research groups, both experimentally[8−12] and theoretically.[13−20] $MgSO_4$ is the main component of seawater responsible for high sound absorption[21] and has been used to protect cellulose during oxygenated delignification.[22] It is also a potential candidate for storing energy in thermal storage systems[23] and is the drug par excellence for the treatment of pregnant women with preeclampsia,[24] among other applications.

It is well-known that $MgSO_4$ associates in the form of ionic pairs in aqueous solutions.[25] Atkinson and Petrucci,[8] using ultrasonic absorption, confirmed that the association equilibrium of ion pairs goes through a three-step mechanism (called the Eigen mechanism), as shown below:

$$\underset{\text{free ions}}{Mg^{+2}(aq) + SO_4^{-2}(aq)} \rightleftharpoons \underset{\text{2SIP}}{[Mg(WW)SO_4]} \rightleftharpoons \underset{\text{SIP}}{[Mg(W)SO_4]} \rightleftharpoons \underset{\text{CIP}}{[MgSO_4]}$$

In this scheme, free ions associate to form a solvent-separated ion pair (2SIP), where two water layers (WW) separate them. The loss of a water molecule in the ion coordination layer (W) generates a solvent-shared ion pair (SIP). Finally, the contact ion pair (CIP) is formed when another water molecule is lost and a Mg−OSO_3 bond appears. Dielectric[10,11] and Raman[9] spectroscopy studies of $MgSO_4$ solutions confirmed the presence of these species. On the other hand, Cao et al.[12] using X-ray diffraction found that SO_4^{-2} coordinates Mg^{2+} in a monodentate fashion (CIP) with

Received: May 29, 2024
Revised: August 7, 2024
Accepted: August 9, 2024
Published: August 17, 2024

a characteristic Mg−S distance of 3.40 Å in concentrated aqueous solutions of $MgSO_4$.

$MgSO_4$ has been widely studied for its antioxidant activity against LP of cell membranes.[26−32] It has been found that this salt protects cell membranes from oxidative damage caused by hydroxyl radicals (•OH) and decreases the LP levels in *in vivo*[28,33,34] and *in vitro*[28,31] experiments. However, the action mechanism of its antioxidant activity is not well established.

In a previous study,[18] it was demonstrated through molecular dynamics and electronic structure calculations how this salt may protect the cell membrane from oxidative damage. It was found that Mg in $MgSO_4$ (CIP) prefers to interact with •OH rather than a water molecule through a direct Mg−OH bond. This interaction is characterized by a relatively strong bond between •OH and Mg of about 70 kcal/mol with changes in the charge and spin density over the OH and sulfate. When •OH is bonded to Mg^{2+}, it loses spin density and gains an electronic charge, and the spin density becomes localized over a pair of sulfate oxygen atoms. This suggests that the unpaired electron is now mainly delocalized on double-bonded oxygens of sulfate. Therefore, the high mobility and reactivity of •OH decreases because they are trapped by the $MgSO_4$, preventing oxidation reactions of lipids and proteins that alter its structures and properties.

In this context, the $MgSO_4$ salt can react with •OH to form a complex in which the unpaired electron is stabilized by resonance at the sulfate oxygens, acting as a shield against •OH by trapping them. This has been confirmed experimentally because several researchers have found that this salt is a •OH scavenger.[22,35−37] Thus, the $MgSO_4$-•OH complexes, which are more stable and less reactive, are expected to recombine with other radicals, restricting the interaction with the membrane lipids and, in this way, mitigating cellular oxidation.

In biological systems, the generation of •OH is substantial. It is estimated that between 1000 and 10 000 •OH are produced per second in each cell under normal conditions.[38] The •OH is the most reactive radical produced in biological systems because it presents a highly positive reduction potential.[39] Therefore, the production of •OH under oxidative stress conditions must be much higher. On the other hand, Akilan et al.[11] found that only 3% of the $MgSO_4$ concentrations used in clinical trials and treatments[40] are in the CIP form at 25 °C. In contrast, the sum of SIP and 2SIP in those conditions represents 30%. This suggests that the hydration structure in which sulfate does not coordinate directly to Mg (SIP and 2SIP) also makes an important contribution to the antioxidant activity exhibited by this salt.

In the present work, the antioxidant properties of $MgSO_4$ against •OH were studied by analysis of the •OH interactions with all $MgSO_4$ ion pairs (CIP, SIP, and 2SIP) using the density functional theory (DFT) approach. The process of spin-electron transfer was determined by studying the spin density, molecular structure, and energetics. Two novel phenomena are observed: the spin transfer from •OH to sulfate at long distances, especially in the SIP and 2SIP structures, and a spin transfer without a direct •OH−Mg interaction.

This work is organized as follows: section 2 shows the proposed molecular configurations of hydrated $MgSO_4$ ion pairs with •OH, the DFT functional used, and the simulation and visualization software implemented. Section 3 addresses the general modification of the structures and electronic properties, the energetic changes in the spin density transfer process, and the comparison of the results obtained with those reported in the literature. Finally, the main findings and future work are presented in section 4.

2. METHODOLOGY

In a previous work,[18] the interaction of $MgSO_4$ in CIP ($5H_2O$) form with •OH was evaluated, using several electronic structure methods (DFT) to analyze the reaction viability between these species. It was proposed that the H abstraction by the •OH from a water molecule coordinated to Mg based on the mechanism of •OH reactive diffusion through water molecules.[41,42] In order to obtain a further detailed description of the $MgSO_4$−•OH interaction, the three ion pairs of $MgSO_4$ (CIP, SIP, and 2SIP) are considered in this work by using 12 water molecules to represent the solvation waters. Initially, the $MgSO_4$ ion pair structures with •OH outside the first Mg coordination sphere were fully optimized with DFT calculations in their electronic ground states. Subsequently, a distance scan point-by-point between the O(•OH) and the H of one of the water molecules coordinated to Mg while all others coordinated were allowed to optimize for minimizing the energy was carried out from ∼2 to ∼1 Å to simulate the H transfer.

Due to the continuous development of methods based on DFT, a literature revision was performed with the aim of selecting a robust and computationally accessible functional and its basis sets. In these senses, the ωB97M-D4[43] functional and the ma-def2-TZVPP[44] basis set have an adequate balance between their robustness and computational efficiency. In this sense, the ωB97M-D4[43] functional is presented as an updated version of the ωB97M-V[45] functional with the Grimme's DFT-D4[46] empirical dispersion, proposed by Najibi and Goerigk. Generally speaking, it has been shown to be superior to ωB97M-V, and it is computationally more economical since the dispersion is not determined in the SCF step. In the case of the basis set, the ma-def2-TVZPP is recommended for general-purpose applications of DFT.[44]

Unrestricted calculations have been applied for all systems because of the unpaired electrons in •OH. To prevent a proton transfer in CIP and SIP, found in a previous work,[19] the solvation model based on density (SMD) method[47] was used to optimize the geometry of all ion pairs. Different types of properties were studied to describe the interactions of these systems: distances, spin density, natural charges on OH and sulfate,[48] and energy differences between the ion pairs in different configurations. All calculations were performed with the ORCA package,[49,50] and visualizations were completed with the VMD software.[51]

3. RESULTS AND DISCUSSION

The results of the distance scan of the H transfer and subsequent constraint-free geometry optimization revealed an intermediate structure in which the spin-electron is transferred without the •OH being coordinated to Mg in all ion pair structures. Therefore, the resulting conformations are characterized by the position of the OH (OHout, nonbonded to Mg, and OHin, bonded to Mg) and spin density (spinOH, spin in OH, and $spinSO_4$, spin in SO_4). In this sense, three types of stable conformations are established, as shown in Figure 1 for CIP $MgSO_4(12H_2O)$ with •OH: (a) OHout/spinOH, where OH is not coordinated with Mg and the spin density is in •OH. (b) OHout/$spinSO_4$, in which OH is not coordinated with Mg

https://doi.org/10.1021/acsomega.4c05053
ACS Omega 2024, 9, 36640−36647

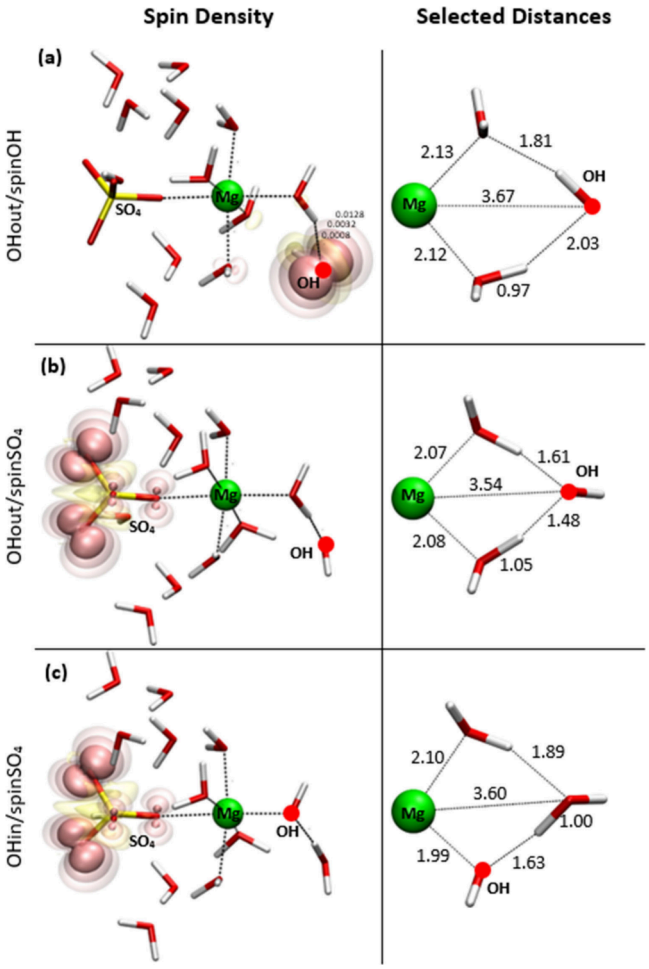

Figure 1. Schematic representation of CIP $MgSO_4(12H_2O)$ with $^{\bullet}OH$ in different stable conformations described by the OH (OHout and OHin) and spin density (spinOH and $spinSO_4$) positions. (a) OHout/spinOH conformation, where OH is not coordinated to Mg and the spin density is over OH. (b) OHout/$spinSO_4$ conformation, in which OH is not coordinated to Mg and the spin density is over sulfate. (c) OHin/$spinSO_4$ conformation, where OH is coordinated to Mg and the spin density is over sulfate. Left, molecular structures and spin density with its isovalues. Right, selected O−Mg and O−H distances are highlighted in Å. Atoms colored red, white, and yellow are O, H, and S atoms, respectively. The green balls represent Mg atoms. Red dots highlight the O($^{\bullet}OH$) atoms.

and the spin density is in sulfate. (c) OHin/$spinSO_4$, where OH is coordinated with Mg and the spin density is in sulfate.

The right side of Figure 1 shows the selected (O−Mg and O−H) interatomic distances, highlighting that in Figure 1a, the Mg−OH distance is 3.67 Å and the spin density is in the OH. However, at the Mg−OH distance of 3.54 Å, the spin density is over the sulfate; see Figure 1b. Here, a stable structure is found with a spin density on sulfate without a direct Mg−$^{\bullet}OH$ bond (OHout/$spinSO_4$ conformation). In Figure 1c, the formation of the HO−Mg bond is observed at a distance of 1.99 Å, which is shorter than that of standard H_2O−Mg (2.12 Å). These conformations are explored in more detail for all ion pairs of $MgSO_4(12H_2O)$−$^{\bullet}OH$ systems in the following section.

3.1. General Overview: Structural and Electronic Properties of Ion Pairs. Figure 2 shows the differences between all ion pairs, the calculated structures, the charges on sulfate and OH, the O−O bond orders, and the spin densities for $MgSO_4(12H_2O)$ with $^{\bullet}OH$ in CIP, SIP, and 2SIP and considering the OHout/spinOH, OHout/$spinSO_4$, and OHin/$spinSO_4$ conformations. For the CIP structures, the sulfate coordinates to Mg in a monodentate manner (Figure 2a−c). In the case of SIP, only one oxygen from the sulfate forms a hydrogen bridge with one Mg-coordinated water (see dashed-dotted lines in Figure 2d−f). In 2SIP, the two water layers that set apart the sulfate from the Mg are clearly observed (see dashed-dotted rectangles in Figure 2g−i).

Table 1 shows selected interatomic distances of all of the systems depicted in Figure 2. For the OHout/spinOH conformations, the S−O($^{\bullet}OH$) distance increases (6.56, 8.27, and 10.50 Å for CIP, SIP, and 2SIP, respectively) with the expected enlargement of the Mg−S distance (3.36, 5.03, and 6.79 Å for CIP, SIP, and 2SIP, respectively). Conversely, the Mg−O($^{\bullet}OH$) and O_s−O_s distances are approximately the same for all ion pairs, with CIP having the shortest Mg−O($^{\bullet}OH$) distance.

The approximation of $^{\bullet}OH$ to Mg from 3.67, 3.76, and 3.76 Å in OHout/spinOH to 3.54, 3.58, and 3.60 Å for OHout/$spinSO_4$ conformations (see second row in Table 1) leads to changes in the spin density in the oxygen atom from the $^{\bullet}OH$ (see Figure 2a,d,g) which is essentially transferred to a pair of oxygens from the sulfate (see Figure 2b,e,h). To verify that spin transfer does not occur due to a lack of solvation on sulfate, $MgSO_4$ CIP with $^{\bullet}OH$ in OHout/$spinSO_4$ and OHin/$spinSO_4$ conformations was calculated with 18 water molecules that cover the sulfate region. Calculations at the PBEh-3c[52] level with implicit solvation (SMD) showed that the spin transfer to sulfate also occurs.

The evaluation of the electronic density shows that an electronic charge transfer between the sulfate and $^{\bullet}OH$ occurs. The sulfate charge reduced from −1.82, −1.84, and −1.86 in CIP, SIP, and 2SIP to −0.95, and the charge in $^{\bullet}OH$ increased from 0.00 to −0.80 (see charge values in red and blue colors for sulfate and OH in Figure 2, respectively). This is reflected in a small increase of the O_s−O_s distances (see the fourth row in Table 1). Also, there is a slightly increase in the Mg−S and S−O($^{\bullet}OH$) distances for CIP (from 3.36 to 3.40 Å and from 6.56 to 6.65 Å, respectively) and SIP (from 5.03 to 5.14 Å and from 8.27 to 8.51 Å, respectively) but a decrease for 2SIP (from 6.79 to 6.73 Å and from 10.50 to 10.26 Å, respectively). However, a notable change occurs within the oxygens with spin density of O_s−O_s(spin), where the distance is shortened from approximately 2.45 to 2.20 Å (see fourth and fifth rows in Table 1). This distance reduction is reflected in a Mayer's bond order index of around 0.30 (see values in black indicated by a black arrow in Figure 2), suggesting that there is a small bonding interaction between these oxygen atoms.

The results shown in Figure 2b,e,h are of great relevance since they indicate a long-distance spin-electron transfer of up to 10 Å from S of sulfate to O of $^{\bullet}OH$ (see the third row in Table 1). The transfer can occur not only in SIP and 2SIP, where sulfate is separated from Mg by water layers (5.03 and 6.79 Å for SIP and 2SIP, respectively), but also with the $^{\bullet}OH$ outside the coordination sphere of Mg. Notice also that the small reduction (around 0.13−0.18 Å) in the Mg−O($^{\bullet}OH$) distance from 3.67−3.76 Å in the OHout/spinOH conformation to 3.54−3.60 Å in the OHout/$spinSO_4$ conformation (see the second row of Table 1) produces the spin transfer from $^{\bullet}OH$ to SO_4 for all ion pairs.

https://doi.org/10.1021/acsomega.4c05053
ACS Omega 2024, 9, 36640−36647

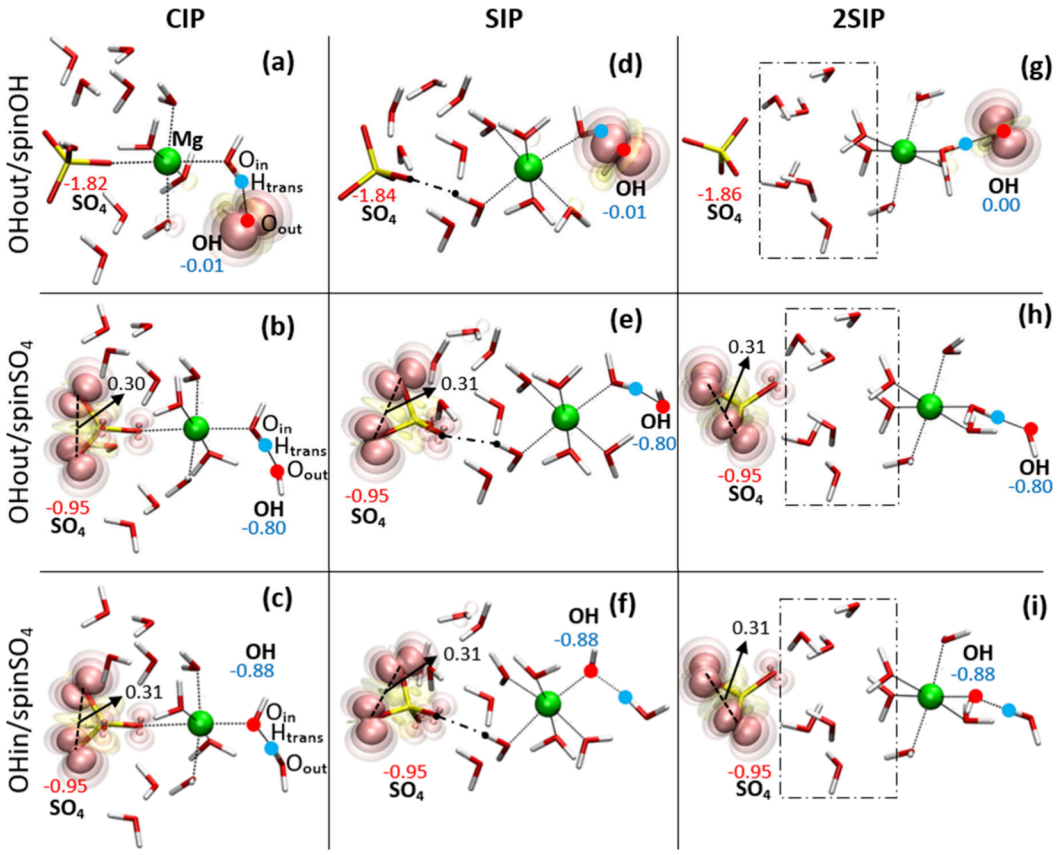

Figure 2. Molecular structures and spin density for $MgSO_4(12H_2O)$ ionic pairs (CIP, SIP, and 2SIP) with •OH in different stable conformations (OHout/spinOH, OHout/spinSO_4, and OHin/spinSO_4). (a) CIP OHout/spinOH. (b) CIP OHout/spinSO_4. (c) CIP OHin/spinSO_4. (d) SIP OHout/spinOH. (e) SIP OHout/spinSO_4. (f) SIP OHin/spinSO_4. (g) 2SIP OHout/spinOH. (h) 2SIP OHout/spinSO_4. (i) 2SIP OHin/spinSO_4. O_{in}, O_{out}, and H_{trans} are atom labels: oxygen coordinated to Mg, oxygen out of Mg coordination sphere, and hydrogen interacting with both oxygens, respectively. Red and blue dots highlight the O(•OH) and H_{trans} atoms, respectively. Natural charge values are indicated in red and blue numbers for sulfate and OH, respectively. Mayer's O–O bond order indexes in sulfate are indicated in black numbers with a black arrow.

Table 1. Calculated Distances for $MgSO_4(12H_2O)$ Ion Pairs (CIP, SIP, and 2SIP) with •OH in Different Stable Conformations (OHout/spinOH, OHout/spinSO_4, and OHin/spinSO_4)

	OHout/spinOH			OHout/spinSO_4			OHin/spinSO_4		
distance (Å)	CIP	SIP	2SIP	CIP	SIP	2SIP	CIP	SIP	2SIP
Mg–S	3.36	5.03	6.79	3.40	5.14	6.73	3.48	5.00	6.78
Mg–O(•OH)[a]	3.67	3.76	3.76	3.54	3.58	3.60	1.99	2.00	2.00
S–O(•OH)[a]	6.56	8.27	10.50	6.65	8.51	10.26	5.44	6.70	8.39
O_s–O_s[b]	2.42	2.42	2.43	2.44	2.45	2.45	2.45	2.45	2.45
O_s–O_s(spin)[c]	–	–	–	2.20	2.19	2.20	2.19	2.20	2.20
Mg–O_{in}[d]	2.12	2.12	2.11	2.08	2.10	2.09	1.99	2.00	2.00
H_{trans}–O_{in}[d]	0.97	0.97	0.97	1.05	1.03	1.03	1.63	1.60	1.61
H_{trans}–O_{out}[d]	2.03	2.08	2.03	1.48	1.54	1.54	1.00	1.01	1.01

[a]O(•OH) = oxygen of hydroxyl radical. [b]O_s–O_s = average sulfate oxygen distances. [c]O_s–O_s(spin) = sulfate oxygens with spin density, as shown in Figure 1. [d]See atom labels in Figure 2a–c.

The direct substitution of a coordination water by •OH also causes a spin density transfer to the sulfate oxygens. However, the charge over •OH increases from −0.80 to −0.88 (see blue values for OH in Figure 2b,e,h and those in Figure 2c,f,i, respectively), and the Mg–O(•OH) distances are shorter than those of OHout configurations (from 3.54–3.60 Å to 1.99–2.00 Å, see second row of Table 1). This means that the interaction between •OH and Mg is stronger, which suggests that these systems are stabilized when •OH is coordinated to Mg. It should be noted, however, that the S–O(•OH) distances are reduced (see the third row in Table 1; from 6.65, 8.51, and 10.26 Å to 5.44, 6.70, and 8.39 Å for CIP, SIP, and 2SIP, respectively).

The comparison of some distances associated with the spin-electron transfer in the $MgSO_4$–•OH conformations, Mg–O_{in}, H_{trans}–O_{in}, and H_{trans}–O_{out}, are also given (see sixth, seventh, and eighth rows in Table 1; see Figure 2 for the atom descriptions). In general, these distances are approximately the same for all three ion pairs in each conformation. It can be proposed that a spin-electron transfer will take place first, followed by a proton transfer from a water molecule (W):

https://doi.org/10.1021/acsomega.4c05053
ACS Omega 2024, 9, 36640−36647

$$(SO_4^{-2}W_n)Mg^{+2}\cdots HO_{in}H_{trans}\cdots {}^{\bullet}O_{out}H \xrightarrow{e^-_{transfer}} ({}^{\bullet}SO_4^{-1}W_n)Mg^{+2}\cdots HO_{in}H_{trans}\cdots O_{out}{}^{-1}H \xrightarrow{H^+_{transfer}} ({}^{\bullet}SO_4^{-1}W_n)Mg^{+2}{-}HO_{in}{}^{-1} + H_{trans}O_{out}H \ (n = 11)$$

For the OHout/spinOH conformations, the $H_{trans}-O_{out}$ distance is a relatively long hydrogen bond (2.03−2.08 Å), and the $H_{trans}-O_{in}$ and $Mg-O_{in}$ distances are typical of the H_2O bonding (0.97 Å) and $Mg-H_2O$ coordination (around 2.12 Å), respectively. When spin density is transferred (OHout/spinSO_4 conformations), the distance between Mg and the coordinated H_2O decreases slightly ($Mg-O_{in}$, from around 2.12 to 2.09 Å), while the $H_{trans}-O_{out}$ distance shortens (on average, from 2.05 to 1.52 Å) and the $H_{trans}-O_{in}$ elongates (from 0.97 to 1.04 Å, approximately), indicating the formation of a strong hydrogen bond, suggesting the preparation for a proton transfer. Finally, when H_{trans} (proton) is transferred (OHin/spinSO_4 conformations), the $Mg-O_{in}$ distance is further shortened (around 2.00 Å), representing an ion−ion $Mg^{2+}-OH^{-1}$ interaction. The resulting $OH^{-1}-H_2O$ hydrogen bond is slightly weaker concerning the OHout/spinSO_4 conformations (on average, from 1.04 to 1.01 Å for the covalent bond and from 1.52 to 1.61 Å for the hydrogen bond).

3.2. Energetics. To analyze the energy change of ion pairs in different configurations, Figure 3 shows the energies of

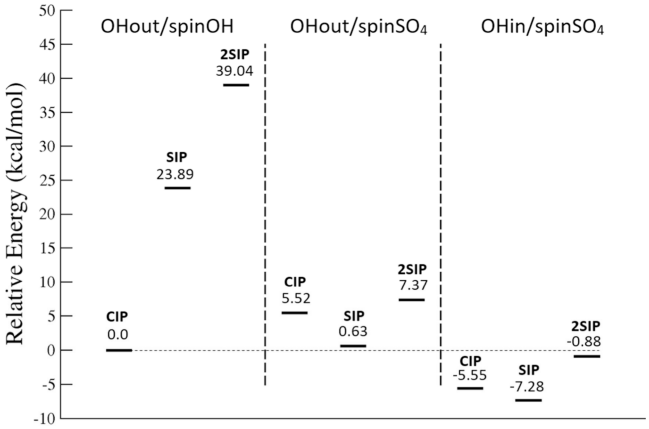

Figure 3. Relative energies of $MgSO_4(12H_2O)$ ion pairs (CIP, SIP, and 2SIP) with $^{\bullet}OH$ in different stable conformations (OHout/spinOH, OHout/spinSO_4, and OHin/spinSO_4) with respect to CIP in the OHout/spinOH configuration.

$MgSO_4(12H_2O)$ ion pairs with $^{\bullet}OH$ relative to those of the CIP OHout/spinOH system. Results show that, in the case of the OHout/spinOH conformation, the SIP and 2SIP have sequentially higher energy than CIP. This correlates with the distance between Mg^{2+} and SO_4^{-2} ions. The longer the Mg−S distance (see the first row in Table 1), the lesser the attractive electrostatic interaction energy. This explains the order CIP < SIP < 2SIP in terms of energy.

When the spin-electron transfer from $^{\bullet}OH$ to sulfate occurs (OHout/spinSO_4 conformations), the energies between the ionic pairs become close to each other with the SIP having the lowest energy. Although they are of higher energy than the CIP OHout/spinOH system, for SIP and 2SIP, the energy decreases considerably (−23.24 and −31.67 kcal/mol for SIP and 2SIP in Figure 3, respectively). In the case of OHin/spinSO_4 conformations, all ion pairs became more stable, showing negative energy values as compared to the CIP OHout/spinOH system, highlighting the large stabilization for the solvent-mediated ion pairs (−5.55, −31.17, and −39.92 kcal/mol for CIP, SIP, and 2SIP in Figure 3, respectively).

These results can be explained by the redistribution of the electrostatic energies. The loss of the sulfate charge causes a decrease in its internal electrostatic repulsion and also significantly weakens its attractive interaction with Mg^{2+}, especially in the CIP case, thus probably causing the energy between the three ion pairs to be similar. The further decrease in energy between the OHout/spinSO_4 and OHin/spinSO_4 conformations is associated with the increase in the attractive energy due to the reduction of the $Mg^{2+}-OH^{-1}$ distance. Lastly, the balance between $SO_4^{-1}-Mg^{2+}$ attraction and $SO_4^{-1}-OH^{-1}$ repulsion is responsible for the change in the distribution of structural stabilities between ionic pairs (SIP < CIP < 2SIP), where the SIP is the most stable structure.

These findings illustrate the energetic electrostatic forces that drive spin-electron transfer even in the absence of direct contact between sulfate and Mg. Likewise, the three ion pairs in spinSO_4 conformations (OHin/spinSO_4 and OHout/spinSO_4) have small energy differences (less than 7 kcal/mol, see Figure 3) suggesting that transfer can occur to any of them. The stabilization in these models indicates that the antioxidant property of $MgSO_4$ is due to a decrease of the $^{\bullet}OH$ reactivity by transforming it into OH^{-1} through a spin-electron transfer.

3.3. Discussion. In a previous work,[18] the possible mechanism of the antioxidant activity of magnesium sulfate in the CIP form was explained through the spin transfer to the sulfate as a result of an electron transfer to $^{\bullet}OH$ stabilizing the unpaired electron by resonance on the S=O bonds of sulfate. However, the results of this work show that spin transfer produces a large electrostatic stability, which is also feasible for all ionic pairs, including those separated by several water layers, as shown in Figure 3. Even more, this transfer occurs without $^{\bullet}OH$ being directly coordinated to Mg. Thus, spin-electron transfer does not require a direct $^{\bullet}OH-Mg$ interaction.

Experimental results reported by Zucchetti et al.[53] showed the electric field modulation of spin transport in the development of spintronic devices within a solid-state environment. They found that the induction of an electric field can alter the diffusion distance of a spin. The spin transport can be modulated by an electric field guiding spins over macroscopic distances, and the spin-diffusion velocity can increase the spin-transport length along a path in germanium. In this direction, the electric field produced by the ionic pairs of $Mg^{2+}-SO_4^{-2}$ can induce spin-electron transfer when $^{\bullet}OH$ is at a certain distance of Mg across the hydrogen bridges of water (see in Figure 2 the comparison in spin densities in OHout/spinOH to those in OHout/spinSO_4 conformations).

The formation of the Mg−OH bond could take place in three steps. In the first step, a spin-electron transfer occurs from the SO_4^{-2} (donor), which is transformed into $^{\bullet}SO_4^{-1}$, where the spin density is delocalized over S=O bonds, and the $^{\bullet}OH$ (acceptor) evolves into OH^{-1}, being more stable because now the oxygen atom obeys the octet rule. In the second step, a proton transfer from a water molecule coordinated to Mg to the outer OH^{-1} occurs, resulting in the formation of a water molecule and an inner OH^{-1}. In the third step, the direct interaction between OH^{-1} and Mg^{2+} produces a relatively strong ionic $Mg-OH^{-1}$ bond shown in the OHin/spinSO_4

https://doi.org/10.1021/acsomega.4c05053
ACS Omega 2024, 9, 36640−36647

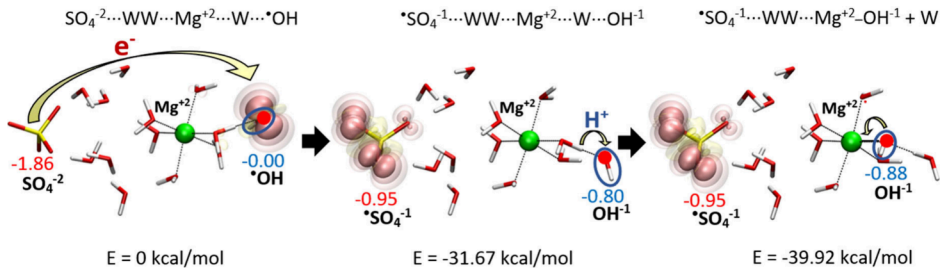

Figure 4. Molecular scheme of spin-electron transfer between SO_4^{-2} and •OH, followed by a proton transfer from a Mg-coordinated water molecule to the outer OH^{-1} for the $MgSO_4$ 2SIP ($12H_2O$) system.

conformations. A schematic of this process is shown in Figure 4.

Electron transfers are one of the most fundamental processes in physics, chemistry, and biology. Biological electron transfer reactions are one of the key steps underlying cellular energy harvesting and storage that are required for respiration[54] and redox reactions of intermediary metabolism.[55] Such reactions are classified into two mechanisms: the inner-sphere mechanism, in which a ligand is shared between two centers acting as a bridge for the electron transfer, and the outer-sphere mechanism, which involves a transfer of electrons between two centers without a bridging ligand.[56] Concerning the proposed scheme, the first mechanism may occur in the CIP, and the second one can be assigned to SIP and 2SIP.

Particularly, outer-sphere electron transfer reactions have been reported for enzymes in the literature in which the donor and the acceptor centers are separated by up to 15 Å.[57,58] In this sense, several authors have published water-mediated electron transfer over long distances, implying its important role in the electron transfer process. de la Lande et al.[59] showed that water molecules are directly involved in the transfer between two metal copper centers separated by 11 Å in peptidylglycine α-hydroxylating monooxygenase. On the other hand, Martin and Matyushov[60] found that the increase in the electron transfer rate of NADH:ubiquinone oxidoreductase by allowing structural water to occupy the protein pocket is produced by the electrowetting of iron−sulfur cofactors that are separated by up to 14 Å. In that respect, Hecker et al.[61] reported the presence of water molecules H-bonded at the tyrosyl radical intermediates in the long-range (32 Å) radical transfer of $\alpha_2\beta_2$-ribonucleotide reductase, confirming the role of water in the electron transfer chain.

In general, the formation of the $MgSO_4$−•OH complex with all ionic pairs is feasible and of great relevance since the solutions of $MgSO_4$ for medical purposes are 4 mM.[40] At this concentration, the percentages of ionic pairs where Mg is separated from sulfate (SIP and 2SIP) are the most important. In medicine, the action of $MgSO_4$ in human beings exposed to high oxidative stress is present in ischemia-reperfusion associated with serious clinical manifestations (myocardial hibernation, acute heart failure, cerebral and gastrointestinal dysfunction, and systemic inflammatory response and multiple organ dysfunction syndromes),[62] including as well as in the uteroplacental circuit during early onset preeclampsia.[63] A possible explanation for the mechanism of action of the treatment of ischemia-reperfusion injury with i.v. infusions of $MgSO_4$ relies on our findings. In this regard, we have found that this salt, when adsorbed on the surface of cell membranes in its different ionic pairs, acts as a shield against the action of •OH radicals.[18] These radicals would otherwise react with the unsaturated hydrocarbon chains in lipids of cellular membranes to oxidize them. The behavior of $MgSO_4$, which forms the $MgSO_4$−•OH complex with all of its ionic pairs, undoubtedly contributes to more effective cellular mechanisms for repairing oxidized membranes.

4. CONCLUSIONS AND COMMENTS

In the present work, the interaction of •OH with different hydrated structures of magnesium sulfate has been studied to better understand the antioxidant properties of this salt. Internuclear bond distances, atomic natural charge, spin density locations, and energy differences between different ion pairs in different configurations were evaluated. The main conclusions are presented below:

(a) In general, the interaction of •OH−Mg produces a spin-electron transfer from the sulfate to the •OH, in which a negative charge appears on •OH and the charge on the sulfate decreases by half. This occurs for all ion pairs.

(b) The approach of a •OH radical to a water molecule coordinated to Mg results in a spin density shift from OH to sulfate without the •OH being directly coordinated to Mg. This indicates that spin density transfer between •OH and SO_4^{-2} may also occur over long distances of up to 10 Å.

(c) The exchange of a Mg-coordinated water by the OH^{-1} further stabilizes the radical with respect to the conformations in which the OH^{-1} is outside the Mg^{2+} solvation sphere because the Mg−OH bond is stronger than Mg−OH_2.

(d) Based on these results, it can be proposed that for all $MgSO_4$ ion pairs, the approach of •OH to Mg causes a spin-electron transfer from sulfate to OH, which is followed by a proton transfer from a Mg-coordinated water molecule to the formed OH^{-1}, producing H_2O plus a OH^{-1} bonded to Mg^{2+}.

(e) The antioxidant properties of $MgSO_4$ are explained by the larger stability of the new radial located on sulfate, which is stabilized by resonance with an equally distributed spin density on the oxygen atoms. This is supported by important electrostatic attractive interactions between Mg^{2+} with OH^{-1} and •SO^{-1} and the electronic repulsion decrease within the sulfate.

Future work will focus on other magnesium salts such as gluconate,[26,64,65] citrate,[36] malate,[36] and threonate[66,67] that have been reported in the literature to have an important antioxidant capacity. It is important to know, in those cases, the mechanism of radical stabilization. In the case of $MgSO_4$, it will also be relevant to the determination of barriers for spin-electron transfer reactions from OHout/spinOH to OHout/

https://doi.org/10.1021/acsomega.4c05053
ACS Omega 2024, 9, 36640−36647

spinSO_4 conformations. In addition, it would also be important to evaluate a $MgSO_4$−water molecular model where free ions are considered to see if there is a limit in distance for this spin-electron transfer phenomenon.

AUTHOR INFORMATION

Corresponding Author

Miguel Fernández − *Laboratorio de Química Computacional, Centro de Química, Instituto Venezolano de Investigaciones Científicas (IVIC), Caracas 1020A, Venezuela;* orcid.org/0000-0002-2203-3829; Email: miguel2158@gmail.com

Authors

Reinaldo Marín − *Laboratorio de Bioenergética Celular, Centro de Biofísica y Bioquímica, Instituto Venezolano de Investigaciones Científicas (IVIC), Caracas 1020A, Venezuela*

Fernando Ruette − *Laboratorio de Química Computacional, Centro de Química, Instituto Venezolano de Investigaciones Científicas (IVIC), Caracas 1020A, Venezuela*

Complete contact information is available at: https://pubs.acs.org/10.1021/acsomega.4c05053

Notes

The authors declare no competing financial interest.

ACKNOWLEDGMENTS

The authors thank the supercomputing infrastructure of the NLHPC (ECM-02), Chile, for the computational time that was generously provided. The authors also thank Miguel Diaz and Alexander Peraza for the fruitful discussions.

REFERENCES

(1) Pizzino, G.; Irrera, N.; Cucinotta, M.; Pallio, G.; Mannino, F.; Arcoraci, V.; Squadrito, F.; Altavilla, D.; Bitto, A. Oxidative Stress: Harms and Benefits for Human Health. *Oxid Med. Cell Longev* **2017**, *2017*, 8416763.

(2) Ashok, A.; et al. Antioxidant Therapy in Oxidative Stress-Induced Neurodegenerative Diseases: Role of Nanoparticle-Based Drug Delivery Systems in Clinical Translation. *Antioxidants* **2022**, *11*, 408.

(3) Patel, R.; Rinker, L.; Peng, J.; Chilian, W. M. Reactive Oxygen Species: The Good and the Bad. In *Reactive Oxygen Species (ROS) in Living Cells*; InTech, 2018. DOI: 10.5772/intechopen.71547.

(4) Yin, H.; Xu, L.; Porter, N. A. Free Radical Lipid Peroxidation: Mechanisms and Analysis. *Chem. Rev.* **2011**, *111*, 5944−5972.

(5) Pleshchitser, A. La. Biological Role of Magnesium. *Clin Chem.* **1958**, *4*, 429−451.

(6) Villa-Bellosta, R. Dietary magnesium supplementation improves lifespan in a mouse model of progeria. *EMBO Mol. Med.* **2020**, *12*, e12423.

(7) Fiorentini, D.; Cappadone, C.; Farruggia, G.; Prata, C. Magnesium: Biochemistry, Nutrition, Detection, and Social Impact of Diseases Linked to Its Deficiency. *Nutrients* **2021**, *13*, 1136.

(8) Atkinson, G.; Petrucci, S. Ion association of magnesium sulfate in water at 25°. *J. Phys. Chem.* **1966**, *70*, 3122−3128.

(9) Rudolph, W. W.; Irmer, G.; Hefter, G. T. Raman spectroscopic investigation of speciation in MgSO4(aq). *Phys. Chem. Chem. Phys.* **2003**, *5*, 5253.

(10) Buchner, R.; Chen, T.; Hefter, G. Complexity in "Simple" Electrolyte Solutions: Ion Pairing in MgSO 4 (aq). *J. Phys. Chem. B* **2004**, *108*, 2365−2375.

(11) Akilan, C.; Rohman, N.; Hefter, G.; Buchner, R. Temperature Effects on Ion Association and Hydration in MgSO4 by Dielectric Spectroscopy. *ChemPhysChem* **2006**, *7*, 2319−2330.

(12) Cao, L.-d.; Fang, Y.; Fang, C.-h. Structure of MgSO4 in Concentrated Aqueous Solutions by X-Ray Diffraction. *Chem. Res. Chin Univ* **2011**, *27* (3), 490−495.

(13) Chaban, G. M.; Huo, W. M.; Lee, T. J. Theoretical study of infrared and Raman spectra of hydrated magnesium sulfate salts. *J. Chem. Phys.* **2002**, *117*, 2532−2537.

(14) Zhang, X.; Zhang, Y.; Li, Q. Ab initio studies on the chain of contact ion pairs of magnesium sulfate in supersaturated state of aqueous solution. *Journal of Molecular Structure: THEOCHEM* **2002**, *594*, 19−30.

(15) Zhang, X. c.; Zhang, Y. h.; Li, Q. s. Ab Initio and DFT Study of Magnesium Sulfate Contact Ion Pairs. *Journal of Beijing Institute of Technology* **2003**, *12* (2), 190−193.

(16) Zhang, H.; Zhang, Y.; Wang, F. Theoretical understanding on the v 1 -SO42− band perturbed by the formation of magnesium sulfate ion pairs. *J. Comput. Chem.* **2009**, *30*, 493−503.

(17) Iype, E.; et al. DFT Study on Characterization of Hydrogen Bonds in the Hydrates of MgSO 4. *J. Phys. Chem. C* **2012**, *116*, 18584−18590.

(18) Fernández, M.; Marín, R.; Proverbio, F.; Chiarello, D. I.; Ruette, F. Magnesium sulfate against oxidative damage of membrane lipids: A theoretical model. *Int. J. Quantum Chem.* **2017**, *117*, No. e25423.

(19) Fernández, M.; Klapp, J.; Sigalotti, L. D. G.; Ruette, F. Hydration study of $MgSO_4$ using different theoretical and model approaches. Is there a proton transfer? *Chem. Phys. Lett.* **2018**, *713*, 39−45.

(20) Fernández, M.; Marín, R.; Proverbio, F.; Ruette, F. Effect of magnesium sulfate in oxidized lipid bilayers properties by using molecular dynamics. *Biochem Biophys Rep* **2021**, *26*, 100998.

(21) Millero, F. J. In *The Physical Chemistry of Natural Waters*; Wiley-Interscience, New York, NY, USA, 2001.

(22) Bouchard, J.; Wang, J.; Berry, R. MgSO4 vs. Mg(OH)2 as a cellulose protector in oxygen delignification. *Holzforschung* **2011**, *65* (3), 295−301.

(23) van Essen, V. M.; Zondag, H. A.; Gores, J. C.; Bleijendaal, L. P. J.; Bakker, M.; Schuitema, R.; van Helden, W. G. J.; He, Z.; Rindt, C. C. M. Characterization of MgSO4 Hydrate for Thermochemical Seasonal Heat Storage. *J. Sol Energy Eng.* **2009**, *131* (4), 041014.

(24) Korish, A. a. Magnesium sulfate therapy of preeclampsia: an old tool with new mechanism of action and prospect in management and prophylaxis. *Hypertens Res.* **2012**, *35*, 1005−11.

(25) Eigen, M.; Tamm, K. Schallabsorption in Elektrolytlösungen als Folge chemischer Relaxation I. Relaxationstheorie der mehrstufigen Dissoziation. *Zeitschrift für Elektrochemie* **1962**, *66*, 93−107.

(26) Marín, R.; et al. Magnesium salts in pregnancy. *Journal of Trace Elements and Minerals* **2023**, *4*, 100071.

(27) Chiarello, D. I.; et al. Mechanisms of the effect of magnesium salts in preeclampsia. *Placenta* **2018**, *69*, 134−139.

(28) Abad, C.; et al. Magnesium sulfate affords protection against oxidative damage during severe preeclampsia. *Placenta* **2015**, *36*, 179−185.

(29) Chiarello, D. I.; et al. Effect of Hypoxia on the Calcium and Magnesium Content, Lipid Peroxidation Level, and Ca 2+ -ATPase Activity of Syncytiotrophoblast Plasma Membranes from Placental Explants. *Biomed Res. Int.* **2014**, *2014*, 1−9.

(30) Abad, C.; et al. Effect of Magnesium Sulfate on the Osmotic Fragility and Lipid Peroxidation of Intact Red Blood Cells from Pregnant Women with Severe Preeclampsia. *Hypertens Pregnancy* **2010**, *29*, 38−53.

(31) Gutiérrez, P.; et al. Ca-ATPase Activity of Human Red Cell Ghosts: Preeclampsia, Lipid Peroxidation and MgSO4. *Hypertens Pregnancy* **2009**, *28*, 390−401.

(32) Abad, C.; et al. Effect of magnesium sulfate on the calcium-stimulated adenosine triphosphatase activity and lipid peroxidation of red blood cell membranes from preeclamptic women. *Biochem. Pharmacol.* **2005**, *70*, 1634−1641.

(33) Maulik, D.; et al. Post-hypoxic magnesium decreases nuclear oxidative damage in the fetal guinea pig brain. *Brain Res.* **2001**, *890*, 130−136.
(34) Ariza, A. C.; et al. Effects of magnesium sulfate on lipid peroxidation and blood pressure regulators in preeclampsia. *Clin Biochem* **2005**, *38*, 128−33.
(35) Thordstein, M.; Bagenholm, R.; Thiringer, K.; Kjellmer, I. Scavengers of free oxygen radicals in combination with magnesium ameliorate perinatal hypoxic-ischemic brain damage in the rat. *Pediatr. Res.* **1993**, *34*, 23−26.
(36) Szentmihályi, K.; Szilágyi, M.; Balla, J.; Ujhelyi, L.; Blázovics, A. In vitro antioxidant activities of magnesium compounds used in food industry. *Acta Aliment* **2014**, *43*, 419−425.
(37) Huang, H.; Hu, Y.; Zhang, H.; Cao, S.; Ma, X. Limitations on the protective action of MgSO4 for cellulose during kraft pulp oxygen delignification. *Bioresources* **2020**, *16*, 1438−1452.
(38) Halliwell, B.; Gutteridge, J. M. C. In *Free Radicals in Biology and Medicine*; Oxford University Press, Oxford, UK, 2015.
(39) Buettner, G. R. The Pecking Order of Free Radicals and Antioxidants: Lipid Peroxidation, α-Tocopherol, and Ascorbate. *Arch. Biochem. Biophys.* **1993**, *300*, 535−543.
(40) Connolly, E.; Worthley, L. I. Intravenous magnesium. *Crit Care Resusc* **1999**, *1*, 162−172.
(41) Codorniu-Hernández, E.; Kusalik, P. G. Mobility Mechanism of Hydroxyl Radicals in Aqueous Solution via Hydrogen Transfer. *J. Am. Chem. Soc.* **2012**, *134*, 532−538.
(42) Iglev, H.; Fischer, M. K.; Gliserin, A.; Laubereau, A. Ultrafast Geminate Recombination after Photodetachment of Aqueous Hydroxide. *J. Am. Chem. Soc.* **2011**, *133*, 790−795.
(43) Najibi, A.; Goerigk, L. DFT-D4 counterparts of leading meta-generalized-gradient approximation and hybrid density functionals for energetics and geometries. *J. Comput. Chem.* **2020**, *41*, 2562−2572.
(44) Zheng, J.; Xu, X.; Truhlar, D. G. Minimally augmented Karlsruhe basis sets. *Theor. Chem. Acc.* **2011**, *128*, 295−305.
(45) Mardirossian, N.; Head-Gordon, M. ωB97M-V: A combinatorially optimized, range-separated hybrid, meta-GGA density functional with VV10 nonlocal correlation. *J. Chem. Phys.* **2016**, *144*, 214110.
(46) Caldeweyher, E.; Ehlert, S.; Hansen, A.; Neugebauer, H.; Spicher, S.; Bannwarth, C.; Grimme, S. A generally applicable atomic-charge dependent London dispersion correction. *J. Chem. Phys.* **2019**, *150*, 154122.
(47) Marenich, A. V.; Cramer, C. J.; Truhlar, D. G. Universal Solvation Model Based on Solute Electron Density and on a Continuum Model of the Solvent Defined by the Bulk Dielectric Constant and Atomic Surface Tensions. *J. Phys. Chem. B* **2009**, *113*, 6378−6396.
(48) Glendening, E. D.; Landis, C. R.; Weinhold, F. NBO 7.0: New vistas in localized and delocalized chemical bonding theory. *J. Comput. Chem.* **2019**, *40*, 2234.
(49) Neese, F. The ORCA program system. *Wiley Interdiscip Rev. Comput. Mol. Sci.* **2012**, *2*, 73−78.
(50) Neese, F. Software update: The ORCA program system - Version 5.0. *WIREs Computational Molecular Science* **2022**, *12*, e1606.
(51) Humphrey, W.; Dalke, A.; Schulten, K. VMD: Visual molecular dynamics. *J. Mol. Graph* **1996**, *14*, 33−38.
(52) Grimme, S.; Brandenburg, J. G.; Bannwarth, C.; Hansen, A. Consistent structures and interactions by density functional theory with small atomic orbital basis sets. *J. Chem. Phys.* **2015**, *143*, 054107.
(53) Zucchetti, C.; Marchionni, A.; Bollani, M.; Ciccacci, F.; Finazzi, M.; Bottegoni, F. Electric field modulation of spin transport. *APL Mater.* **2022**, *10*, 011102.
(54) Hirst, J. Mitochondrial Complex I. *Annu. Rev. Biochem.* **2013**, *82*, 551−575.
(55) Zoccarato, A.; Nabeebaccus, A. A.; Oexner, R. R.; Santos, C. X. C.; Shah, A. M. The nexus between redox state and intermediary metabolism. *FEBS J.* **2022**, *289*, 5440−5462.
(56) Arnaut, L. Electron-transfer reactions. In *Chemical Kinetics*; Elsevier, 2021; p 523−577. DOI: 10.1016/B978-0-444-64039-0.00001-7.
(57) Winkler, J. R.; Gray, H. B. Electron transfer in ruthenium-modified proteins. *Chem. Rev.* **1992**, *92*, 369−379.
(58) Gray, H. B.; Winkler, J. R. Electron tunneling through proteins. *Q. Rev. Biophys.* **2003**, *36*, 341−372.
(59) de la Lande, A.; Martí, S.; Parisel, O.; Moliner, V. Long Distance Electron-Transfer Mechanism in Peptidylglycine α-Hydroxylating Monooxygenase: A Perfect Fitting for a Water Bridge. *J. Am. Chem. Soc.* **2007**, *129*, 11700−11707.
(60) Martin, D. R.; Matyushov, D. V. Electron-transfer chain in respiratory complex I. *Sci. Rep.* **2017**, *7*, 5495.
(61) Hecker, F.; Stubbe, J.; Bennati, M. Detection of Water Molecules on the Radical Transfer Pathway of Ribonucleotide Reductase by ^{17}O Electron−Nuclear Double Resonance Spectroscopy. *J. Am. Chem. Soc.* **2021**, *143*, 7237−7241.
(62) Wu, M.-Y.; et al. Current Mechanistic Concepts in Ischemia and Reperfusion Injury. *Cellular Physiology and Biochemistry* **2018**, *46*, 1650−1667.
(63) Marín, R.; et al. Oxidative stress and mitochondrial dysfunction in early-onset and late-onset preeclampsia. *Biochimica et Biophysica Acta (BBA) - Molecular Basis of Disease* **2020**, *1866*, 165961.
(64) Rojas, D.; Abad, C.; Piñero, S.; Medina, Y.; Chiarello, D. I.; Proverbio, F.; Marín, R. Effect of Mg-Gluconate on the Osmotic Fragility of Red Blood Cells, Lipid Peroxidation, and Ca2+-ATPase (PMCA) Activity of Placental Homogenates and Red Blood Cell Ghosts From Salt-Loaded Pregnant Rats. *Front. Physiol.* **2022**, *13*, 794572.
(65) Rangel, H.; Abad, C.; Chiarello, D. I.; Rojas, D.; Proverbi, F.; Marín, R. Can magnesium gluconate be used as an alternative therapy for preeclampsia? *Physiological Mini Reviews* **2022**, *15*, 39−48.
(66) Huang, Y.; et al. Magnesium boosts the memory restorative effect of environmental enrichment in Alzheimer's disease mice. *CNS Neurosci Ther* **2018**, *24*, 70−79.
(67) Shen, Y.; et al. Treatment Of Magnesium-L-Threonate Elevates The Magnesium Level In The Cerebrospinal Fluid And Attenuates Motor Deficits And Dopamine Neuron Loss In A Mouse Model Of Parkinson's disease. *Neuropsychiatr Dis Treat* **2019**, *15*, 3143−3153.

https://doi.org/10.1021/acsomega.4c05053
ACS Omega 2024, 9, 36640−36647